



HAL
open science

New series of acridines and phenanthrolines: synthesis and characterization

Amel Souibgui, Anne Gaucher, Jérôme Marrot, Flavien Bourdreux, Faouzi Aloui, Bechir Ben Hassine, Damien Prim

► **To cite this version:**

Amel Souibgui, Anne Gaucher, Jérôme Marrot, Flavien Bourdreux, Faouzi Aloui, et al.. New series of acridines and phenanthrolines: synthesis and characterization. Tetrahedron, 2014. hal-02973885

HAL Id: hal-02973885

<https://hal.uvsq.fr/hal-02973885>

Submitted on 21 Oct 2020

HAL is a multi-disciplinary open access archive for the deposit and dissemination of scientific research documents, whether they are published or not. The documents may come from teaching and research institutions in France or abroad, or from public or private research centers.

L'archive ouverte pluridisciplinaire **HAL**, est destinée au dépôt et à la diffusion de documents scientifiques de niveau recherche, publiés ou non, émanant des établissements d'enseignement et de recherche français ou étrangers, des laboratoires publics ou privés.

Graphical Abstract

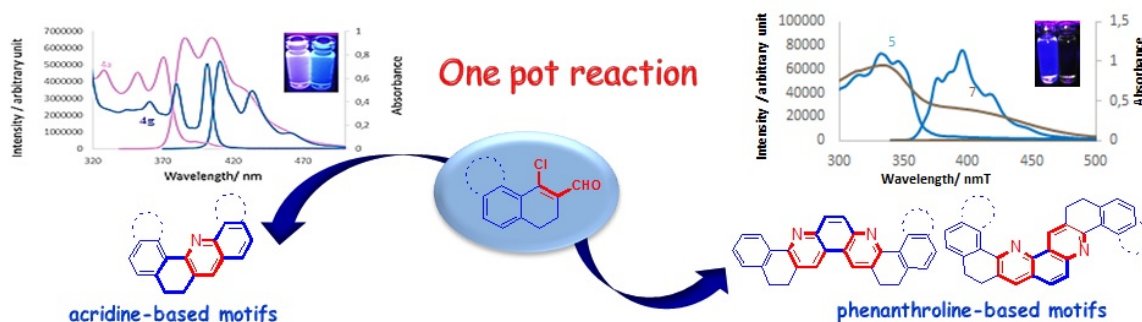
New series of acridines and phenanthrolines: synthesis and characterization.

Leave this area blank for abstract info.

Amel Souibgui,^{a,b} Anne Gaucher,^a Jérôme Marrot,^a Flavien Bourdreux,^a Faouzi Aloui,^b Bechir Ben Hassine,^{b*} and Damien Prim^{a*}

^a *University of Versailles Saint-Quentin-en-Yvelines, Institut Lavoisier de Versailles UMR CNRS 8180, 45, avenue des Etats-Unis, 78035 Versailles cedex, France*

^b *Laboratoire de Synthèse Organique, Asymétrie et Catalyse Homogène. Faculté des sciences de Monastir, Avenue de l'Environnement, 5019 Monastir, Tunisia*





New series of acridines and phenanthrolines: synthesis and characterization.

Amel Souibgui,^{a,b} Anne Gaucher,^a Jérôme Marrot,^a Flavien Bourdreux,^a Faouzi Aloui,^b Bechir Ben Hassine,^{b*} and Damien Prim^{a*}

^a University of Versailles Saint-Quentin-en-Yvelines, Institut Lavoisier de Versailles UMR CNRS 8180, 45, avenue des Etats-Unis, 78035 Versailles cedex, France

^b Laboratoire de Synthèse Organique, Asymétrie et Catalyse Homogène. Faculté des sciences de Monastir, Avenue de l'Environnement, 5019 Monastir, Tunisia

ARTICLE INFO

Article history:

Received

Received in revised form

Accepted

Available online

Keywords:

Acridine-based architectures
phenanthrolines

ABSTRACT

New series of acridines and phenanthrolines have been prepared from β -chlorovinyl aldehydes and various aniline derivatives allowing the installation of valuable substituents such as ketone, nitro or amino groups at the heterocyclic core. X-ray analyses confirmed the structures of acridines and phenanthrolines as well as the presence of partially hydrogenated rings and their crucial impact on the overall shape of the acridine-based architectures. ¹H NMR revealed the helical behaviour of several acridine motives. Comparison of UV data between architectures and influence of number of partially hydrogenated rings is also described.

2009 Elsevier Ltd. All rights reserved.

1. Introduction

Acridine is an aromatic linear tricyclic motif comprising a central pyridine and two fused benzene rings. Known for more than one century, this heterocycle and its derivatives is still of great interest in the scientific community. Indeed, they represent an appealing structural feature widely occurring in numerous natural products with biological activities and in medicinal chemistry. For instance, acridine-based compounds recently showed anti-malarial,¹ -microbial,² -inflammatory,³ -cancer⁴ and acetylcholinesterase inhibition⁵ activities.

The acridine motif can also be found in chemosensors, dyes, fluorescent probes,⁶ as ligands in metal-promoted catalysis⁷ or very recently in hole transport or chiroptical materials⁸ and two photon absorption devices.⁹ Most of these properties are strongly dependent on the combination of two main factors¹⁰ that are (i) the nature of substituents and their specific interactions with proteins, lipids, DNA or natural macromolecules and (ii) the crucial role of the acridine-platform nitrogen atom. Current strategies developed to increase and/or modulate the

forementioned properties rely first on the extension of the aromatic motif through additional benzo- or naphtho-fused rings that may generate various linear and angular topologies.¹¹ The incorporation of a second nitrogen atom leading to the phenanthroline family and to a new range of specific properties represents a second research line.¹² The fine tuning of the overall flexibility of the acridine platform through incorporation of partially hydrogenated cycles within the acridine core is an additional emerging concern.¹³ Nevertheless, catalytic hydrogenation on substituted acridine structures does not necessarily give access to partially hydrogenated moieties. It appears to be dependent on the position of the substituent.¹⁴ A more convenient approach should be the construction of acridine derivatives from partially saturated precursors. Slight structural modifications from entirely aromatic to partially hydrogenated shape have been shown to bring significant changes in pharmaceutical activities¹⁵ and to induce novel photophysical properties.¹⁶ Elaboration of methodologies that allow the joint construction of new acridine-based topologies, the control of structural parameters such as the presence of partially hydrogenated ring and the installation of additional nitrogen atoms are challenging and worthwhile.

We have recently reported on the preparation and influence of structural modulations on photophysical properties of fused fluorenones including acridino-fluorenones.¹⁷ The high efficiency of our strategy, encouraged us to explore the construction of new acridine series that allows (i) the installation of various fused rings (benzo, dibenzo, naphtho) to the acridine motif, (ii) the

* Corresponding authors. Tel.: +331-39-25-44-54; fax: +331-39-25-44-52; e-mail: damien.prim@uvsq.fr. (Damien prim) Tel.: +216-735-00278; e-mail: bechir.benhassine@fsm.mu.tn. (Béchir Ben Hassine).

regiodefined introduction of nitrogen atoms, (iii) the comparison of physical properties between partially hydrogenated and fully aromatic structures. We thus report herein the preparation of new acridines as well as [1,7]- and [4,7]-phenanthrolines, that incorporate partially hydrogenated ring using a single and easy-to-set strategy (Fig. 1). NMR as well as X-ray support the determination of novel topologies. Comparison of photophysical data is also given showing the impact of structural modulations on UV/Vis, fluorescence and band gap energies.

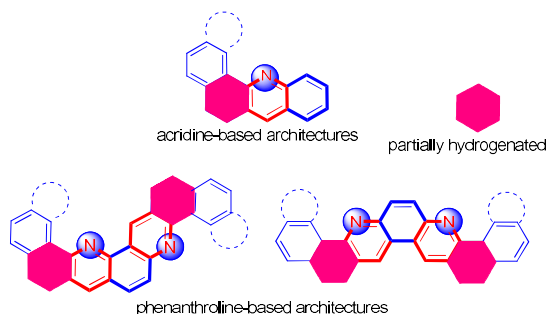


Figure 1. Example of targeted acridine-based topologies.

2. Results and discussion

We first started with the preparation of various acridines from β -chlorovinyl aldehydes. As recently reported by us,¹⁸ aldehydes **1** and **2** were readily obtained from the parent cycloalkanone derivatives (Fig. 2).

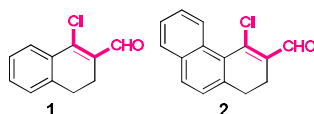
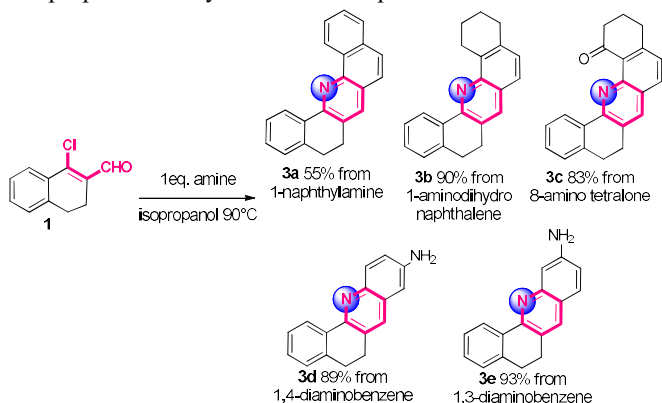


Figure 2. Starting β -chlorovinyl aldehydes.

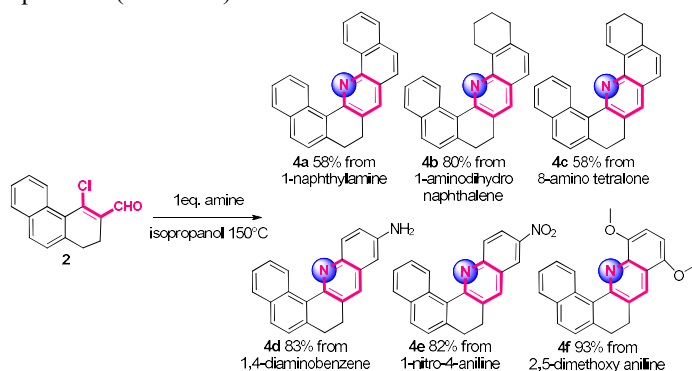
The reaction of anilines with β -chlorovinyl aldehydes for the preparation of heterocycles including quinolines and more scarcely acridines, has already been reported.¹⁹ Having in view the construction of elaborated targets, the use of large excess of the reacting amine (up to 5 equivalents) or metal mediated processes as well as the tedious isolation of the intermediates as stated in these former studies appeared less attractive and inclined us to revisit the preparation of acridine-based motives and define our own conditions. Gratifyingly, reaction of equimolar amounts of **1** and various anilines at 90°C in isopropanol cleanly afforded the expected acridines **3**.



Scheme 1. Preparation of various dihydroacridines from β -chlorovinyl aldehyde **1**.

The use of concentrations ranging from 0.1-0.13 mol.L⁻¹ avoided the formation of side products and limited the purification step to a simple filtration or recrystallization (scheme 1). As shown in scheme 1, high to quantitative yields were obtained regardless of the reacting amine. Indeed, 1-naphthylamine, 1-amino dihydronaphthalene, 8-amino tetralone, 1,4-diaminobenzene and 1,3-diaminobenzene afforded compounds **3a-e** respectively. Interestingly, no trace of potential bisadduct was observed when 1 eq. of 1,4-diaminobenzene was used. Similarly, **3e** was obtained as the unique product starting from **1** and 1,3-diaminobenzene. Compound **3e** results from a selective construction of the pyridine ring through preferred cyclization at the less congested aromatic site. Noteworthy, one or two fused benzene rings, an additional saturated cycle or functions such as amino and ketone groups can be selectively appended to the linear tricyclic dihydroacridine core.

Our strategy was next extended to β -chlorovinyl aldehydes **2**. Similar conditions (1 eq. amine, isopropanol) were used for the preparation of acridine derivatives **4a-e**. Heating at 150°C ensured completion of reactions and high yields of expected products (Scheme 2).



Scheme 2. Preparation of various dihydroacridines from β -chlorovinyl aldehydes **2**.

Reaction of 1-naphthylamine, 1-amino dihydronaphthalene and 1,4-diaminobenzene with **2** afforded acridine derivatives **4a-b** and **4d** which are benzofused analogues of **3a-b** and **3d** respectively. This series could be extended to anilines bearing an electron withdrawing group such as nitro without significant decrease of yield. In contrast to **3c**, the reaction involving 8-aminotetralone did not lead to the expected ketone. In fact, **4c** was isolated in a fair 58% yield. No satisfactory explanation could be given for the plausible overall “reduction-elimination” process observed under such conditions. Single crystals of **3b** and **4b** were obtained by slow evaporation of a dichloromethane solution. Solid state analysis confirmed the molecular structure of both acridine derivatives (Fig. 3).

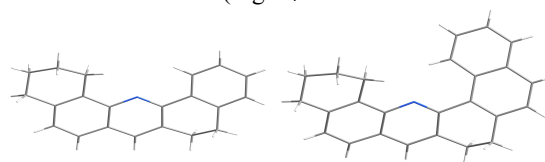


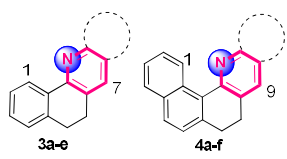
Figure 3. X-ray structure determination of **3b** (left) and **4b** (right).²⁰

Both structures confirm the presence of dihydro units in the fused polycyclic architecture. The overall architecture displays a twisted geometry resulting from the presence of one or two cyclohexyl units. An almost planar central quinoline is

accommodated by two cyclohexyl units at each side. Within these cyclohexyl rings, contiguous methylene carbons lay up and beneath the median plane of each aromatic fragment, both contributing to the overall molecular distortion. As shown, the major effect is observed in **4b** which comprises one naphthalene instead of one benzene unit.

Selected ^1H NMR data are gathered in table 1. Interestingly, chemical shifts for H(1) and H(7) in **3a-e** and H(1) and H(9) in **4a-f** are characteristic of the dihydroacridine substitution pattern. Indeed, chemical shifts of both H(1) and H(7) in **3a-e**, that arise from β -chlorovinyl aldehyde **1**, are impacted by the presence of strong electron donating group. A decrease of chemical shifts from 8.68 to 8.51 and 8.54 is observed for NH_2 substituents (**3d** and **3e**) by comparison with cyclohexyl-fused structure **3b**. In contrast, installation of a ketone or an additional aromatic group led to an increase of the chemical shifts by 0.07 and 0.12 ppm respectively.

Table 1. Selected characteristic ^1H NMR data (δ in ppm) for compounds **3a-e** and **4a-f**.



Compound	$\delta\text{H}(1)$	$\delta\text{H}(7)$	Compound	$\delta\text{H}(1)$	$\delta\text{H}(9)$
3a	8.80	7.95	4a	9.98	8.08
3b	8.68	7.84	4b	10.02	7.94
3c	8.75	7.86	4c	9.88	7.90
3d	8.51	7.67	4d	9.58	7.88
3e	8.54	7.76	4e	9.68	8.17
			4f	9.99	8.41

The presence of an additional ring considerably modifies the ^1H NMR spectra. Indeed, in each structure H(1) undergo a large shielding effect plausibly due to the tight relationship with the nitrogen atom lone pair. $\delta\text{H}(1)$ ranged from 9.58 to 10.02 ppm evidencing a clear trend to helicity behaviour. In contrast, chemical shift of the pyridinic H(9) proton appears less affected by the presence of an additional fused ring. Evolution of the chemical shifts being related to the nature of the substituents, similarly to compounds **3**. Aromatization by mean of DDQ in refluxing toluene led to the fully aromatic molecule **4g** in a 93% yield (Fig. 4).

Moving from the partially hydrogenated **4a** to the fully aromatic **4g** through aromatization process impacts the overall shape of the molecule. Indeed, oxidation process enforces both methylene carbons to reach a planar shape. Comparison of ^1H NMR spectra of compounds **4a** and **4g** undoubtedly account for the evolution of the molecular architecture towards planarity. Protons H(9), H(1) and H(15) are privileged spectators *vis-à-vis* the evolution of the molecular structure. Indeed, the shielding of pyridinic H(9) proton $\Delta\delta = \delta[\text{H}(9) \text{ in } \mathbf{4g}] - \delta[\text{H}(9) \text{ in } \mathbf{4a}]$ is 0.7 ppm. Noteworthy, fjord region protons H(1) and H(15) undergo differently the effect of aromatization process.²¹ H(1) and H(15) are shielded by 1.7 and 0.2 ppm respectively in good agreement

with an increase of helical behaviour. The large shielding observed for H(1) most likely results from the closer relationship with the nitrogen lone pair by contrast with H(15). According to these data, **4g** might be considered as an extended aza-helicene (Fig. 4).

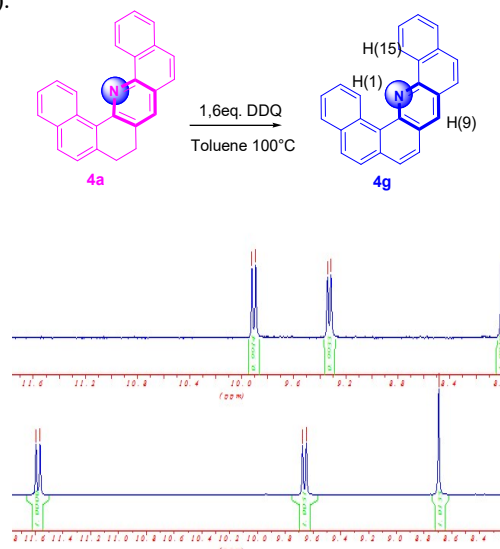


Figure 4. Aromatization and comparison of ^1H NMR spectra between **4a** (up) and **4g** (beneath).

We next evaluated the formation of extended architectures based on a dihydroacridine motif such as [1,7]- and [4,7]-phenanthrolines. Advantageously, the preparation of phenanthrolines was envisioned through either condensation of amino acridine derivatives **3d**, **3e** or **4d** and an additional equivalent of β -chlorovinyl aldehydes or a one pot double condensation using two equivalents of β -chlorovinyl aldehydes and one equivalent of diamino substrate. Within this context, we first examined the reaction of **3d** or **4d** with β -chlorovinyl aldehydes **1** or **2**. As shown below, this condensation may afford one quinacridine (Fig.5, top) or one phenanthroline (Fig.5, bottom) depending on the cyclisation site.

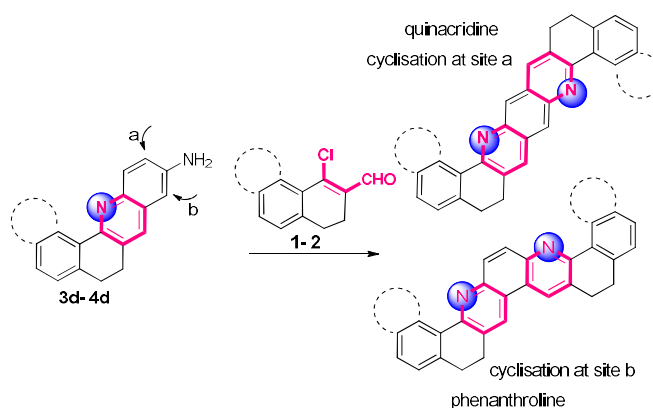


Figure 5. Envisioned access to quinacridine or phenanthroline starting from **1** and **2**.

In fact, this reaction leads only to one product in a high 70% yield. ^1H and ^{13}C NMR confirmed the selective formation of a symmetrical phenanthroline showing characteristic signals and shape of fully symmetrical molecule but did not allow discrimination between both structures. The structure of 13,14,17,18-tetrahydronaphtho[2,1-b:1',2'-j][4,7]phenanthroline **5** was unambiguously assigned through single crystal X-ray analysis as shown in figure 6.

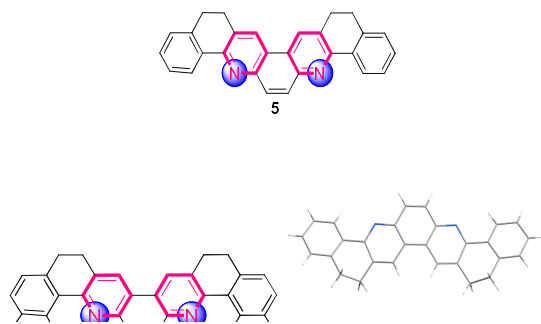
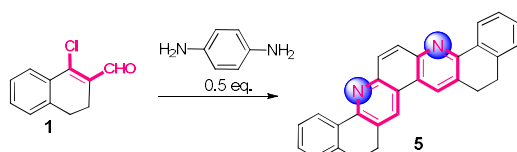


Figure 6. Structural determination of 13,14,17,18-tetrahydrodinaphtho[2,1-b:1',2'-j][4,7]phenanthroline **5** (left) and **6** (right).

As already evidenced, the central almost planar phenanthroline is linked to two benzene rings by saturated cycles partly responsible for the overall shape of the molecule. Surprisingly, only compound **6** displays weak π - π interactions. As shown, π - π interactions (3.68, 3.63 and 3.79 Å) between two terminal naphthalene units and two central heterocycles respectively set the design of trimeric arrangement. Noteworthy, phenanthroline **5** could also be selectively prepared from **1** and 1,4-diaminobenzene through sequential addition of the diamine substrate at 90°C in isopropanol (scheme 3). Similarly, phenanthroline **6** could be obtained starting from **2**.



Scheme 3. Synthesis of phenanthroline **5**.

β -Chlorovinyl aldehyde **1** was further condensed with 1,3-diaminobenzene. Although this condensation may afford one quinacridine and one phenanthroline (Fig. 7), only product **7** was isolated in 29% yield after purification. Careful analysis of ^1H NMR spectra evidenced the presence of singlets resonating at 7.97 and 9.46 ppm that account for protons H(8) and H(16) respectively. The chemical shift of H(8) is consistent with those observed for H(7) in compounds **3** (table 1). Similarly, protons H(4) and H(14) resonate at 8.75 ppm which is in good agreement with analogous protons in compounds **3** (table 1). The large shielding observed for H(16) ($\delta = 9.48$ ppm) might plausibly result from the joint contribution of the pyridine ring and the fjord region nitrogen atom lone pair. COSY as well as NOE experiments show signals characteristic of protons H(7)-H(6), H(17)-H(16) and H(8)-H(9) relationships and allowed us to unambiguously assign the structure of phenanthroline **7**.

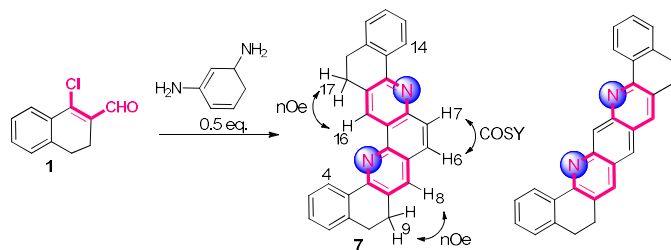


Figure 7. Selective access to phenanthroline **7** starting from **1** and 1,3-diaminobenzene.

Absorption spectra of compounds **3a-b** and **4a-b** were recorded in dilute dichloromethane solutions (Fig. 8). Marked differences can be observed moving from **3b**, to **3a** and further **4a-b**.

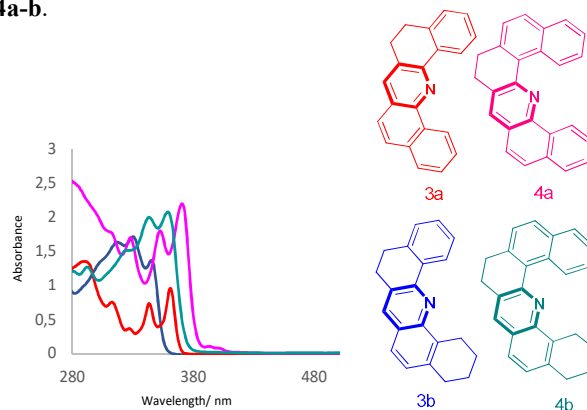


Figure 8. UV/Vis absorption spectra of various acridines in dichloromethane.

As expected, the longest-wavelength hyperchromic absorption maxima of **4a** occur at 372 nm. The latter is redshifted by 25 nm relative to **3a** due to the introduction of an additional fused benzene ring unit leading to an extension of the π conjugation. Decrease of π conjugation either by moving from a naphthalene to a benzene unit (compare **4a** to **3a**), from a benzoquinoline to a quinoline (compare **4a** to **4b**) or combining both (compare **4a** to **3b**) led to ipsochromic shifts of 25, 17, 22 nm respectively.

We next compared both UV/Vis absorption and emission spectra of compounds **4a** and **4g** (Fig. 10).

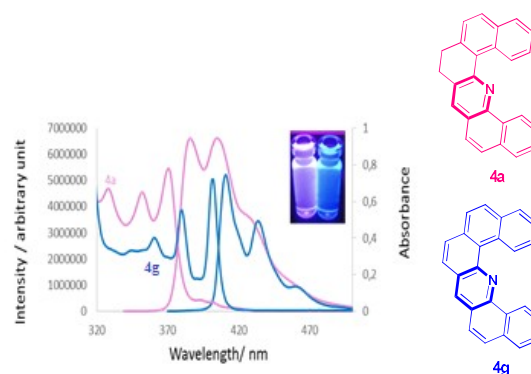


Figure 10. Absorption and emission spectra for compounds **4a** and **4g**.

Both absorption spectra exhibit a set of three bands at 328, 355, 372 nm for **4a** and 360, 381, 403 nm for **4g**. Emission spectra were recorded at 328 and 360 nm respectively and showed similarly two sets of three broad bands at 387, 407, 429 and 411, 435, 463. Bathochromic shifts observed by moving from **4a** to **4g** are in good agreement with a concomitant extension of π conjugation and lesser spatial deformation. Comparison of absorption and emission spectra for **5** and **7**, which only differ each other by the relative nitrogen position pattern, is shown in Figure 10. Phenanthroline **5** displays three absorption bands at 312, 335 and 345 nm and five emission bands (excitation at 335 nm) at 380, 384, 395, 418 and 447 nm. Moving from the symmetrical [4,7]-phenanthroline **5** to the non symmetrical [1,7]-phenanthroline **7** led to noticeable modifications. Indeed, absorption spectra exhibit broad and less

well resolved bands as well as absence of fluorescence (excitation at 338 nm).

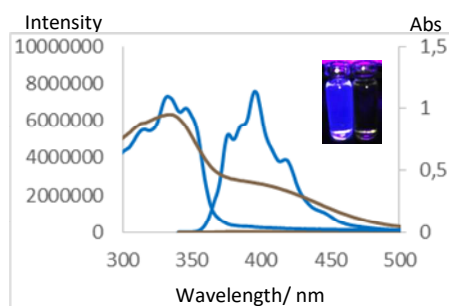


Figure 11. Absorption and emission spectra for phenanthrolines **5** and **7**.

Starting from absorption spectra, we were also able to determine the optical energy band gap (OEBG) of acridines and phenanthrolines, **3a-b**, **4a-b**, **4g**, **6** and **7**.

Table 2. Optical bandgaps for compounds **3a-7**.

Compound	λ_{\max} (nm)	λ_{onset} (nm) ^a	E_g (eV)
3a	347	356	3.50
3b	359	375	3.29
4a	372	395	3.13
4b	355	374	3.33
4g	403	410	3.04
5	342	372	3.35
6	382	396	3.14
7	339	392	3.18

^a The criterion for reading “onset” wavelengths was that the peak absorbance, after background (subtraction) correction, should attain 5% of the absorbance of the lowest-energy wavelength absorption peak.

The OEBG were calculated from the onset of the absorption at 356-479 nm and gathered in table 2. The UV absorption shows that **3a-b**, **4a-b**, **4g**, **6-7** display an OEBG ranging from 3.04 to 3.50 eV. As experimental evidence, we can assume that the OEBG values increase, when the number of cycles in the molecule increases.

3. Conclusion

We have developed a rapid and robust strategy to prepare redefined acridines and phenanthrolines using β -chlorovinyl aldehydes and various aniline derivatives. X-ray analyses confirmed the structures of novel acridines and phenanthrolines and highlighted the crucial impact of the presence of partially hydrogenated rings on the overall shape of the acridine-based architectures. ¹H NMR revealed the presence of characteristic

shifts that are consistent with a trend towards helicity of acridines. A complete UV/Vis study was also achieved, showing that bathochromic shifts were depending on the extension of π -conjugation and the modification of spatial 3D shape of the targets induced by the presence and number of partially hydrogenated rings.

4. Experimental section

4.1. General

Unless otherwise noted, all starting materials were obtained from commercial suppliers and used without purification. Petroleum ether was distilled under Argon. NMR spectra were recorded on a 300 MHz and 200 MHz Bruker spectrometers. Chemical shifts were reported in ppm relative to the residual solvent peak (7.27 ppm for CHCl₃) for ¹H spectra and (77.00 ppm for CDCl₃) for ¹³C spectra. High Resolution Mass spectroscopy data were recorded on an Autospec Ultima (Waters/Micromass) device with a resolution of 5000 RP at 5%. UV/Vis analyses were performed on a Perkin-Elmer spectrophotometer UV/Vis/NIR Lambda 19. A 1 cm path quartz cells were used for the measurements. Steady-state fluorescence measurements were recorded on a spectrofluorimeter FluoroMax-3 equipped with a 150W Xenon lamp and a slit width of 5 nm. For all measurements, the samples used for fluorescence are the same for UV/vis, Infrared spectra were recorded with a FT spectrometer. Compounds **1**, **2** and **3a** were prepared according to literature.^{18, 19} Melting points were determined in open capillary tubes and are uncorrected. Thin-layer chromatography (TLC) was carried out on aluminium sheets precoated with silica gel 60 F254. Column chromatography separations were performed using silica gel (0.040-0.060 mm). X-ray intensity data were collected on a Bruker X8-APEX2 CCD area-detector diffractometer using Mo-K α radiation ($\lambda = 0.71073$ Å). The structure was solved by direct methods, developed by successive difference Fourier syntheses, and refined by full-matrix least-squares on all F₂ data using SHELXTL V6.12.

4.2. General procedures for the synthesis of acridines 3-7.

Dihydroacridines 3a-e: A round-bottom flask was charged under argon with β -chlorovinyl aldehyde **1** (0.5 mmol), amine (0.5 mmol), and dry *isopropanol* (3 mL). The reaction mixture was stirred and heated 90 °C for 2h. After coming back to room temperature, the brown colored organic mass was extracted with dichloromethane (3 x100 mL) and the layers were separated. The organic layer was dried over magnesium sulfate and the solvent was removed under reduced pressure. Thus obtained residue was subjected to column chromatography purification on silica gel.

Dihydroacridines 4a-f: A round-bottom flask was charged under argon with β -chlorovinyl aldehyde **1** (0.5 mmol), amine (0.5 mmol), and dry *isopropanol* (3 mL). The reaction mixture was stirred and heated 150 °C for 2h. After coming back to room temperature, the brown colored organic mass was extracted with dichloromethane (3 x100 mL) and the layers were separated. The organic layer was dried over magnesium sulfate and the solvent was removed under reduced pressure. Thus obtained residue was subjected to column chromatography purification on silica gel.

Acridine 4g: Dihydroacridine **4a** (44 mg, 0.13 mmol) and DDQ (48 mg, 0.21 mmol) were dissolved in toluene (1 mL) and heated at reflux for 3 h. After cooling to room temperature, the resulting solution was purified by flash chromatography eluting with

petroleum ether/ethyl acetate : 98/02 to yield to acridine **4g** as a yellow solid (40 mg, 0.121 mmol, 93%).

Dihydroacridines 5-7: A round-bottom flask was charged under argon with appropriate β -chlorovinyl aldehyde (0.5 mmol), amine (0.25 mmol), and dry *isopropanol* (3 mL). The reaction mixture was stirred and heated 150 °C for 2h. After coming back to room temperature, the brown colored organic mass was extracted with dichloromethane (3 x100 mL) and the layers were separated. The organic layer was dried over magnesium sulfate and the solvent was removed under reduced pressure. Thus obtained residue was subjected to column chromatography purification on silica gel.

4.2.1. 1,2,3,4,8,9-Hexahydrodibenzo[*c,h*]acridine (**3b**).

After purification on silica gel (PE/EtOAc : 90/10), **3b** was obtained (135 mg, 90 %) as a yellow solid. m.p. 128 °C. ¹H NMR (300 MHz, CDCl₃): δ 1.94-2.01 (m, 4 H), 2.96-3.14 (m, 6 H), 3.52 (br., 2 H), 7.20-7.27 (m, 2 H), 7.30-7.52 (m, 3 H), 7.84 (s, 1 H), 8.68 (d, J = 7.5 Hz, 1 H). ¹³C NMR (75 MHz, CDCl₃): δ 23.0, 23.1, 24.7, 28.4, 30.2, 123.8, 125.9, 126.0, 127.1, 127.8, 128.4, 129.1, 129.3, 133.8, 134.8, 135.2, 137.2, 139.2, 146.1, 151.5. HRMS-ESI: m/z [M + H]⁺ calcd for C₂₁H₂₀N: 286.1596; found: 286.1592.

4.2.2. 3,4,8,9-Dihydrodibenzo[*c,h*]acridin-1(2H)-one (**3c**).

After purification on silica gel (CH₂Cl₂ and MeOH/CH₂Cl₂: 50:50), **3c** was obtained (260 mg, 83 %) as a black solid. m.p. 190 °C. ¹H NMR (300 MHz, CDCl₃): δ 2.19-2.27 (m, 2 H), 2.83-2.88 (m, 2 H), 2.98-3.03 (m, 2 H), 3.08-3.13 (m, 4 H), 7.23-7.27 (m, 1 H), 7.30-7.39 (m, 2 H), 7.42-7.47 (m, 2 H), 7.79 (d, J = 8.1 Hz, 1 H), 7.86 (s, 1 H), 8.75 (d, J = 7.3 Hz, 1 H). ¹³C NMR (75 MHz, CDCl₃): δ 23.0, 28.2, 28.4, 31.1, 40.9, 126.8, 126.9, 127.1, 127.6(2), 127.7, 128.5, 129.9, 130.1, 131.8, 133.7, 134.8, 134.9, 139.2, 147.9, 198.3. HRMS-ESI: m/z [M + H]⁺ calcd for C₂₁H₁₈NO: 300.1388; found: 300.1391.

4.2.3. 9-Amino-5,6-dihydrobenzo[*c*]acridine (**3d**).

After purification on silica gel CH₂Cl₂, **3d** was obtained (115 mg, 89 %) as a brown solid. m.p. 52 °C. ¹H NMR (300 MHz, CDCl₃): δ 2.96-3.09 (m, 4 H), 3.85 (br., 2 H), 6.85 (d, J = 2.2 Hz, 1 H), 7.10 (dd, J = 1.8 Hz, J = 8.8 Hz, 1 H), 7.24-7.43 (m, 4 H), 7.67 (s, 1 H), 7.97 (d, J = 8.9 Hz, 1 H), 8.51 (d, J = 7.7 Hz, 1 H). ¹³C NMR (75 MHz, CDCl₃): δ 28.4, 28.8, 107.0, 120.8, 125.4, 127.2, 127.8, 128.9, 129.3, 130.9, 131.7, 131.7, 134.8, 138.8, 142.5, 144.4, 149.9. HRMS-ESI: m/z [M + H]⁺ calcd for C₁₇H₁₅N₂: 247.1235; found: 247.1233.

4.2.4. 10-Amino-5,6-dihydrobenzo[*c*]acridine (**3e**).

After purification on silica gel CH₂Cl₂, **3e** was obtained (120 mg, 93 %) as a brown solid. m.p. 86 °C. ¹H NMR (300 MHz, CDCl₃): δ 2.96-3.05 (m, 4 H), 3.93 (br., 2 H), 6.92 (dd, J = 2.3 Hz, J = 8.7 Hz, 1 H), 7.25-7.42 (m, 4 H), 7.54 (d, J = 8.7 Hz, 1 H), 7.76 (s, 1 H), 8.54 (d, J = 8.7 Hz, 1 H). ¹³C NMR (75 MHz, CDCl₃): δ 28.4, 28.5, 109.6, 118.2, 121.8, 125.9, 127.0, 127.1, 127.8, 127.9, 129.3, 133.6, 134.4, 139.4, 147.0, 149.1, 153.3. HRMS-ESI: m/z [M + H]⁺ calcd for C₁₇H₁₅N₂: 247.1235; found: 247.1237.

4.2.5. 7,8-Dihydrobenzo[*c*]naphtho[1,2-*h*]acridine (**4a**).

After purification on silica gel (PE/CH₂Cl₂ : 90/10), **4a** was obtained (160 mg, 58 %) as a brown solid. m.p. 160 °C. ¹H NMR (300 MHz, CDCl₃): δ 3.13 (br., 4 H), 7.45 (d, J = 8.3 Hz, 1 H), 7.55 (m, 1 H), 7.68-7.95 (m, 8 H), 8.08 (s, 1 H), 9.40 (d, J = 8.1 Hz, 1 H), 9.98 (d, J = 8.7 Hz, 1 H). ¹³C NMR (75 MHz, CDCl₃): δ

28.8, 30.1, 124.6, 124.8, 125.2, 126.4, 127.0, 127.1, 127.4, 127.5, 127.6, 127.8(2), 128.3, 130.1(2), 131.1, 131.9, 133.2, 133.4, 133.5, 134.0, 139.8, 144.5, 153.2. HRMS-ESI: m/z [M + H]⁺ calcd for C₂₅H₁₈N: 332.1439; found: 332.1429.

4.2.6. 7,8,12,13,14,15-Hexahydrobenzo[*c*]naphtho[1,2-*h*]acridine (**4b**).

After purification on silica gel (PE/CH₂Cl₂ : 90/10), **4b** was obtained (110 mg, 80 %) as a brown solid. m.p. : 150 °C. ¹H NMR (300 MHz, CDCl₃): δ 1.94-2.01 (m, 4 H), 2.95-2.99 (m, 2 H), 3.07 (br., 4 H), 3.49-3.53 (m, 2 H), 7.24-7.27 (m, 1 H), 7.42 (d, J = 8.1 Hz, 1 H), 7.49-7.55 (m, 2 H), 7.61-7.66 (m, 1 H), 7.88 (t, J = 8.4 Hz, J = 9.4 Hz, 2 H), 7.94 (s, 1 H), 10.02 (d, J = 6 Hz, 1 H). ¹³C NMR (75 MHz, CDCl₃): δ 23.1, 23.2, 25.1, 28.9, 30.2, 30.3, 123.6, 125.0, 125.1, 126.4, 126.7, 127.9, 128.2, 128.6, 130.0, 130.3, 131.1, 131.5, 133.1, 133.9, 135.1, 137.2, 139.9, 145.9, 153.3. HRMS-ESI: m/z [M + H]⁺ calcd for C₂₅H₂₂N: 336.1752; found: 336.1747.

4.2.7. 7,8,12,13-Dihydrobenzo[*c*]naphtho[1,2-*h*]acridine (**4c**).

After purification on silica gel (PE/CH₂Cl₂ : 90/10), **4c** was obtained (80 mg, 58 %) as a brown solid. m.p. : 138 °C. ¹H NMR (300 MHz, CDCl₃): δ 2.45-2.51 (m, 2 H), 2.99-3.07 (m, 6 H), 6.26-6.32 (m, 1 H), 7.33 (d, J = 8.1 Hz, 1 H), 7.42 (d, J = 8.1 Hz, 1 H), 7.50-7.68 (m, 3 H), 7.85-7.95 (m, 4 H), 9.88 (d, J = 8.7 Hz, 1 H). ¹³C NMR (75 MHz, CDCl₃): δ 23.1, 28.1, 29.0, 30.3, 123.7, 124.8, 125.2, 125.9, 126.4, 126.9, 127.2, 127.8, 128.3, 128.9, 130.2, 130.3, 131.1, 131.2, 131.8, 133.0, 133.9, 135.3, 140.1, 142.7, 153.8. HRMS-ESI: m/z [M + H]⁺ calcd for C₂₅H₂₀N: 334.1596; found: 334.1594.

4.2.8. 11-Amino-7,8-dihydronaphtho[2,1-*c*]acridine (**4d**).

After purification on silica gel CH₂Cl₂, **4d** was obtained (54 mg, 83%) as a brown solid. m.p. : 152 °C. ¹H NMR (200 MHz, CDCl₃): δ 3.03 (br., 4 H), 6.92 (d, J = 2.6 Hz, 1 H), 7.16 (dd, J = 2.6 Hz, J = 7.1 Hz, 1 H), 7.37-7.50 (m, 2 H), 7.53-7.67 (m, 1 H), 7.79-7.88 (m, 3 H), 8.17 (d, J = 8.4 Hz, 1 H), 9.58 (d, J = 8.8 Hz, 1 H). ¹³C NMR (75 MHz, CDCl₃): δ 29.2, 30.1, 106.9, 121.0, 125.3, 126.2, 127.1, 127.2, 128.3, 128.5, 129.7, 129.8, 130.1, 130.9, 131.0, 131.7, 133.3, 133.9, 134.5, 139.7, 144.9. HRMS-ESI: m/z [M + H]⁺ calcd for C₂₁H₁₇N₂: 297.1392; found: 297.1392.

4.2.9. 11-Nitro-7,8-dihydronaphtho[2,1-*c*]acridine (**4e**).

After purification on silica gel CH₂Cl₂, **4e** was obtained (110 mg, 82%) as a yellow solid. m.p. 200 °C. ¹H NMR (200 MHz, CDCl₃): δ 3.13 (br., 4 H), 7.44 (d, J = 8.3 Hz, 1 H), 7.54 (t, J = 6.9 Hz, J = 14.9 Hz, 1 H), 7.67 (tdd, J = 1.2 Hz, J = 8.5 Hz, 1 H), 7.92 (t, J = 8 Hz, J = 16 Hz, 2 H), 8.17 (s, 1 H), 8.31 (d, J = 9.2 Hz, 1 H), 8.42 (d, J = 2.4 Hz, 1 H), 8.74 (d, J = 2.3 Hz, 1 H), 9.68 (d, J = 8.7 Hz, 1 H). ¹³C NMR (75 MHz, CDCl₃): δ 29.0, 29.8, 122.2, 123.5, 125.7(2), 126.3, 127.0, 127.7, 128.5, 128.9, 130.7, 131.1, 131.8, 133.9, 134.4, 135.0, 141.3, 145.2, 148.9, 158.2. HRMS-ESI: m/z [M + H]⁺ calcd for C₂₁H₁₅N₂O₂: 327.1134; found: 327.1127.

4.2.10. 10,13-Dimethoxy-7,8-dihydronaphtho[2,1-*c*]acridine (**4f**).

After purification on silica gel (PE/CH₂Cl₂ : 90/10), **4f** was obtained (65 mg, 93%) as a yellow oil. ¹H NMR (300 MHz, CDCl₃): δ 3.1 (br., 4 H), 4 (s, 3 H), 4.07 (s, 3 H), 6.76 (d, J = 9 Hz, 1 H), 6.93 (d, J = 9 Hz, 1 H), 7.40 (d, J = 6 Hz, 1 H), 7.51 (t, J = 6 Hz, J = 15 Hz, 1 H), 7.65 (t, J = 6 Hz, J = 15 Hz, 1 H), 7.85 (t, J = 6 Hz, J = 15 Hz, 1 H), (s, 1 H), 9.99 (d, J = 6 Hz, 1 H). ¹³C

NMR (75 MHz, CDCl₃): δ 29.1, 30.2, 55.7, 56.3, 103.6, 106.4, 120.0, 125.1, 126.2, 127.4, 127.4, 127.9, 128.2, 129.8, 130.3, 131.4, 132.4, 133.9, 139.0, 139.8, 148.2, 150.0, 153.8. HRMS-ESI: m/z [M + H]⁺calcd for C₂₃H₂₀NO₂: 342.1494; found: 342.1490.

4.2.11. Benzo[*c*]naphtho[1,2-*h*]acridine (**4g**).

After purification on silica gel (PE/ACOEt : 98/02), **4g** was obtained (40 mg, 93%) as a yellow solid. m.p.: 190 °C. ¹H NMR (300 MHz, CDCl₃): δ 7.74-7.88 (m, 4 H), 7.91-8.11 (m, 8 H), 8.69 (s, 1 H), 9.62 (d, J = 8 Hz, 1 H), 11.57 (d, J = 8.8 Hz, 1 H). ¹³C NMR (75 MHz, CDCl₃): δ 124.2, 125.3, 125.7, 126.1, 126.6, 126.7, 127.0, 127.2, 127.4, 127.8, 128.1, 128.4, 128.5, 128.5, 130.0, 131.7, 130.8, 131.7, 132.2, 133.7, 134.1, 134.1, 135.1, 146.1, 147.5. HRMS-ESI: m/z [M + H]⁺calcd for C₂₅H₁₈N: 330.1283; found: 330.1280.

4.2.12. 13,14,17,18-Dihydrodinaphtho[2,1-*b*:1',2'-*jj*][4,7]phenanthroline (**5**).

After purification on silica gel (PE/CH₂Cl₂ : 50/50), **5** was obtained (250 mg, 70%) as a yellow solid. m.p. 260 °C. ¹H NMR (300 MHz, CDCl₃): δ 3.05-3.09 (m, 2 H), 3.21-3.26 (m, 2 H), 7.28-7.47 (m, 3 H), 8.08 (s, 1 H), 8.28 (s, 1 H), 8.62 (d, J = 9.4 Hz, 1 H). ¹³C NMR (75 MHz, CDCl₃): δ 28.2, 28.9, 123.6, 126.0, 127.4, 128.0, 129.9, 130.8, 139.1. HRMS-ESI: m/z [M + H]⁺calcd for C₂₈H₂₁N₂: 385.1705; found: 385.1705.

4.2.13. 17,18,21,22-Tetrahydro[3,4-*b*:4',3'-*jj*][4,7]phenanthroline (**6**).

After purification on silica gel (PE/CH₂Cl₂ : 50/50), **6** was obtained (35 mg, 88%) as a white solid. m.p. 265 °C. ¹H NMR (300 MHz, CDCl₃): δ 3.13-3.21 (m, 4 H), 7.45 (d, J = 8.3 Hz, 1 H), 7.54 (t, J = 7.3, J = 14.8 Hz, 1 H), 7.69 (t, J = 7.8, J = 15.2 Hz, 1 H), 7.88-7.92 (m, 2 H), 8.38 (s, 1 H), 8.77 (s, 1 H), 9.87 (d, J = 8.7 Hz, 1 H). ¹³C NMR (75 MHz, CDCl₃): δ 29.4(2), 30.1(2), 122.7(2), 126.3(2), 126.4(2), 127.3(2), 127.3(2), 128.3(2), 128.5(2), 129.5(2), 130.5(2), 131.1(2), 131.3(2), 133.2(2), 134.0(2), 139.9(2), 146.1(2), 154.7(2). HRMS-ESI: m/z [M + H]⁺calcd for C₃₆H₂₅N₂: 485.2018; found: 485.2013.

4.2.13. 9,10,17,18-Dihydrodinaphtho[1,2-*b*:1',2'-*jj*][1,7]phenanthroline (**7**).

After purification on silica gel (PE/CH₂Cl₂ : 90/10), **7** was obtained (54 mg, 29%) as a yellow solid. m.p. : 92 °C. ¹H NMR (300 MHz, CDCl₃): δ 3.04-3.11 (m, 4 H), 3.16-3.20 (m, 2 H), 3.29-3.33 (m, 2 H), 7.31 (d, J = 7.4 Hz, 1 H), 7.38-7.52 (m, 4 H), 7.84 (d, J = 8.9, 1 H), 7.97 (s, 1 H), 8.16 (d, J = 8.9, 1 H), 8.67 (d, J = 7.4, 1 H), 8.75 (d, J = 7.5, 1 H), 9.48 (s, 1 H). ¹³C NMR (300 MHz, CDCl₃): δ 28.2, 28.3, 28.5, 28.8, 125.4, 125.8, 126.1, 126.3, 127.2, 127.3, 127.9, 128.0, 128.8(2), 129.6, 129.9, 130.1, 130.8, 131.0, 131.2, 131.4, 134.1, 134.8, 139.1, 139.4, 144.2, 152.1, 153.3. HRMS-ESI: m/z [M + H]⁺calcd for C₂₈H₂₁N₂: 385.1705; found: 385.1710.

Acknowledgments

The authors are grateful to Direction Générale de la Recherche Scientifique of the Tunisian Ministry of Higher Education and Scientific Research, to the CNRS and the University of Versailles-St Quentin-en-Yvelines for financial support.

Supplementary Material

Copies of ¹H and ¹³C NMR spectra for all products. Detailed ¹H NMR assignment tables. Supplementary data associated with this article can be found in the online version, at

References and notes

- (a) Yu, X.-M.; Ramiandrasoa, F.; Guetzoyan, L.; Pradines, B.; Quintino, E.; Gabelle, D.; Forterre, P.; Cresteil, T.; Mahy, J.-P.; Pethe, S. *Chem. Med. Chem.* **2012**, *7*, 587-605. (b) Hwang, J. Y.; Kawasuji, T.; Lowes, D. J.; Clark, J. A.; Connelly, M. C.; Zhu, F.; Guiguemde, W. A.; Sigal, M. S.; Wilson, E. B.; De Risi, J. L.; Guy, R. K. *J. Med. Chem.* **2011**, *54*, 7084-7093. (c) Kumar, A.; Srivastava, K.; Raja Kumar, S.; Puri, S. K.; Chauhan, P. M. S. *Bioorg. Med. Chem. Lett.* **2010**, *20*, 7059-7063. (d) Visp, S.; Vandenberghe, I.; Robin, M.; Annereau, J. P.; Crancier, L.; Pique, V.; Galy, J. P.; Kruczynski, A.; Barret, J. M.; Bailly, C. *Biochem. Pharmacol.* **2007**, *73*, 1863-1872.
- (a) Nadaraj, V.; Selvi, S. T.; Mohan, S. *Eur. J. Med. Chem.* **2009**, *44*, 976-980. (b) Demeunynck, M.; Charmantray, F.; Martelli, A. *Curr. Pharm. Des.* **2001**, *7*, 1703-1724.
- (a) Chen, Y.-L.; Chen, I.-L.; Lu, C.-M.; Tzeng, C.-C.; Tsao, L.-T.; Wang, J.-P. *Bioorg. Med. Chem.* **2003**, *11*, 3921-3927. (b) Chen, Y.-L.; Lu, C.-M.; Chen, I.-L.; Tsao, L.-T.; Wang, J.-P. *J. Med. Chem.* **2002**, *45*, 4689-4694.
- (a) Fadeyi, O. O.; Adamson, S. T.; Myles, E. L.; Okoro, C. O. *Bioorg. Med. Chem. Lett.* **2008**, *18*, 4172-4176. (b) Belmont, P.; Bosson, J.; Godet, T.; Tiano, M. *Anti-Cancer Agents Med. Chem.* **2007**, *7*, 139-169.
- Alonso, D.; Dorransoro, I.; Rubio, L.; Munoz, P.; Garcia-Palomero, E.; Del Monte, M.; Bidon-Chanal, A.; Orozco, M.; Luque, F. J.; Castro, A.; Medina, M.; Martinez, A. *Bioorg. Med. Chem.* **2005**, *13*, 6588-6597.
- (a) Marti-Centelles, V.; Burgete, M. I.; Galindo, F.; Izquierdo, M. A.; Kumar, D. K.; White, A. J. P.; Luis, S. V.; Vilar, R. *J. Org. Chem.* **2012**, *77*, 490-500. (b) Ghosh, A. K.; Samanta, A.; Bandyopadhyay, P. *J. Phys. Chem. B* **2011**, *115*, 11823-11830. (c) Jimenez-Millan, E.; Giner-Casares, J. J.; Munoz, E.; Martin-Romero, M. T.; Camacho, L. *Langmuir* **2011**, *27*, 14888-14899. (d) Mahmood, T.; Paul, A.; Ladame, S. *J. Org. Chem.* **2010**, *75*, 204-207. (e) Talwelkar, M.; Pedireddi, V. R. *Tetrahedron Lett.* **2010**, *51*, 6901-6905. (f) Bell, T. W.; Hext, N. M. *Chem. Soc. Rev.* **2004**, *33*, 589-598.
- (a) Gunanathan, C.; Shimon, L. J. W.; Milstein, D. *J. Am. Chem. Soc.* **2009**, *131*, 3146-3147. (b) Gunanathan, C.; Milstein, D. *Angew. Chem., Int. Ed.* **2008**, *47*, 8661-8664. (c) Tong, X.; Xu, J.; Miao, H.; Gao, J. *Tetrahedron Lett.* **2006**, *47*, 1763-1766.
- (a) Kim, M.; Lee, J. Y. *Organic Electronics* **2012**, *13*, 1245-1249. (b) Jierry, L.; Harthong, S.; Aronica, C.; Mulatier, J.-C.; Guy, L.; Guy, S. *Org. Lett.* **2012**, *14*, 288-291. (c) Park, M. S.; Lee, J. Y. *Chem. Mater.* **2011**, *23*, 4338-4343.
- (a) Kamada, K.; Fuku-en, S.-I.; Minamide, S.; Ohta, K.; Kishi, R.; Nakano, M.; Matsuzaki, H.; Okamoto, H.; Higashikawa, H.; Inoue, K.; Kojima, S.; Yamamoto, Y. *J. Am. Chem. Soc.* **2013**, *135*, 232-241. (b) Mackiewicz, N.; Delaire, J. A.; Rutherford, A. W.; Doris, E.; Mioskowski, C. *Chem. Eur. J.* **2009**, *15*, 3882-3888.
- (a) Sarangi, M. K.; Mitra, A.; Basu, S. *J. Phys. Chem. B* **2012**, *116*, 10275-10282. (b) Graham, L. A.; Wilson, G. M.; West, T. K.; Day, C. S.; Kucera, G. L.; Bierbach, U. *ACS Med. Chem. Lett.* **2011**, *2*, 687-691. (c) Collie, G. W.; Sparapani, S.; Parkinson, G. N.; Neidle, S. *J. Am. Chem. Soc.* **2011**, *133*, 2721-2728. (d) Grant, K. B.; Terry, C. A.; Gude, L.; Fernandez, M.-J.; Lorente, A. *Bioorg. Med. Chem. Lett.* **2011**, *21*, 1047-1051. (e) Qi, X.; Xia, T.; Roberts, R. W. *Biochemistry* **2010**, *49*, 5782-5789. (f) Sparapani, S.; Haider, S. M.; Doria, F.; Gunaratnam, M.; Neidle, S. *J. Am. Chem. Soc.* **2010**, *132*, 12263-12272. (g) V. P. Zambre, V. P.; Murumkar, P. R.; Giridhar, R.; Yadav, M. R. *J. Chem. Inf. Model.* **2009**, *49*, 1298-1311.
- (a) Shukla, S. P.; Tiwari, R.; Verma, A. K. *Tetrahedron* **2012**, *68*, 9035-9044. (b) Huang, Z.; Yang, Y.; Xiao, Q.; Zhang, Y.; Wang, J. *Eur. J. Org. Chem.* **2012**, 6586-6593. (c) Cikotaeni, I. *Tetrahedron Lett.* **2009**, *50*, 2570-2572. (d) Belmont, P.; Andrez, J.-C.; Allan, C. S. M. *Tetrahedron Lett.* **2004**, *45*, 2783-2786.
- (a) Singh, B.; Chandra, A.; Singh, R. M. *Tetrahedron* **2011**, *67*, 2441-2446. (b) Kuninobu, Y.; Tatsuzaki, T.; Matsuki, T.; Takai,

- K. *J. Org. Chem.* **2011**, *76*, 7005-7009. (c) Bouffier, L.; Dinica, R.; Debray, J.; Dumy, P.; Demeunynck, M. *Bioorg. Med. Chem. Lett.* **2009**, *19*, 4836-4838. (d) Carta, A.; Loriga, M.; Paglietti, G.; Ferrone, M.; Fermeglia, M.; Pricl, S.; Sanna, T.; Ibba, C.; La Colla, P.; Loddo, R. *Bioorg. Med. Chem.* **2007**, *15*, 1914-1927.
13. (a) Wu, Y.; Zhang, X.-X.; Wang, C.; Zhao, L.-L.; Chen, L.-F.; Liu, G.-X.; Huang, S.-Y.; Yue, S.-N.; Zhang, W.-L.; Wu, H. *Tetrahedron* **2013**, *69*, 3947-3950. b) Liao, S.-R.; Zhou, C.-X.; Wu, W.-B.; Ou, T.-M.; Tan, J.-H.; Li, D.; Gu, L.-Q.; Huang, Z.-S. *Eur. J. Med. Chem.* **2012**, *53*, 52-63. c) Cho, C. S.; Kim, H. B.; Ren, W. X.; Yoon, N. S. *Appl. Organometal. Chem.* **2010**, *24*, 817-820. d) Brahma, S.; Ray, J. K. *Tetrahedron* **2008**, *64*, 2883-2896 and references cited therein. e) Bonacorso, H. G.; Drekenner, R. L.; Rodrigues, I. R.; Vezzosi, R. P.; Costa, M. B.; Martins, M. A. P.; Zanatta, N. *J. Fluor. Chem.* **2005**, *126*, 1384-1389. f) Hesse, S.; Kirsch, G. *Tetrahedron* **2005**, *61*, 6534-6539.
14. Mignon, P.; Tiano, M.; Belmont, P.; Favre-Reguillon, A.; Chermette, H.; Fache, F. *J. Mol. Catal. A: Chem.* **2013**, *371*, 63-69.
15. Nadaraj, V.; Selvi, S. T.; Mohan, S. *Eur. J. Med. Chem.* **2009**, *44*, 976-980.
16. (a) Sahraei, R.; Pordel, M.; Behmadi, H.; Razavi, B. *J. Lumin.* **2013**, *136*, 334-338. (b) Grant, K. B.; Terry, C. A.; Gude, L.; Fernandez, M.-J.; Lorente, A. *Bioorg. Med. Chem. Lett.* **2011**, *21*, 1047-1051.
17. Souibgui, A.; Gaucher, A.; Marrot, J.; Aloui, A.; Mahuteau-Betzer, F.; Ben Hassine, B.; Prim, D. *Eur. J. Org. Chem.* **2013**, 4515-4522.
18. Requet, A.; Souibgui, A.; Pieters, G.; Ferhi, S.; Letaieff, A.; Carlin-Sinclair, A.; Marque, S.; Marrot, J.; Ben Hassine, B.; Gaucher, A.; Prim, D. *Tetrahedron Lett.* **2013**, *54*, 4721-4725.
19. (a) Brahma, S.; Ray, J. K. *Tetrahedron* **2008**, *64*, 2883-2896 and references cited therein. (b) Karthikeyan, P.; Rani, A. M.; Saiganesh, R.; Balasubramanian, K. K.; Kabilan, S. *Tetrahedron* **2009**, *65*, 811-821. (c) Su, Q.; Li, P.; He, M.; Wu, Q.; Ye, L.; Mu, Y. *Org. Lett.* doi.org/10.1021/ol402732n.
20. Compound **3b**: CCDC 957960; compound **4b**: CCDC 957963; compound **5**: CCDC 957961; compound **6**: CCDC 957962.
21. Perez, D.; Pena, D.; Guitian, E. *Eur. J. Org. Chem.* **2013**, 5981-6013.